RESEARCH

RESEARCH: Original Research

3D double-faced interlock fabric triboelectric nanogenerator for bio-motion energy harvesting and as self-powered stretching and 3D tactile sensors

Chaoyu Chen [1,2,†], Lijun Chen [1,2,†], Zhiyi Wu [1,†], Hengyu Guo [1], Weidong Yu [2], Zhaoqun Du [2,∗], Zhong Lin Wang [1,3,∗]

[1] School of Material Science and Engineering, Georgia Institute of Technology, Atlanta, GA 30332, United States
[2] Key Laboratory of Textile Science & Technology, Ministry of Education, College of Textiles, Donghua University, Shanghai 201620, PR China
[3] Beijing Institute of Nanoenergy and Nanosystems, Chinese Academy of Sciences, Beijing 100083, PR China

Combining triboelectric nanogenerator (TENG) and textile materials, wearable electronic devices show great application prospects in biomotion energy harvesting and multifunctional self-power sensors in this coming intelligent era. However, fabrication method by rigidly stitching two or more individual fabrics together and working mode that must cooperate with external materials, make textile-based TENG bulky, stiff, uncomfortable and hinder their range of application. Here, by using a double needle bed flat knitting machine technology, a 3D double faced interlock fabric TENG (3DFIF-TENG) is designed as self-powered, stretchable and substrate-free wearable TENG sensors (such as a bending sensor to detect arm bending degree, pressure sensors) and energy harvesting devices. Besides, due to the unique 3D structure and after improving the structure by knitting a woven fabric-TENG in the middle layer, the 3DFIF-TENG can be further used as a multifunctional sensors, such as a 3D tactile sensor. Besides, by knitting a woven fabric-TENG in the middle layer of the 3DFIF-TENG, it can be further used as a multifunctional sensor, such as a 3D tactile sensor. The substrate-free and 3D structure design in this paper may provide a promising direction for self-powered, stretchable wearable devices in energy harvesting, human motion or robot movement detection, and smart prosthetics.

Introduction

Textile triboelectric nanogenerator (TENG) [1], which combines advantages of textiles for its breathability, washability, flexibility, lightweight [2–5] and TENG for its energy harvesting and versatile sensing ability [6–8], shows great application prospects in the coming intelligent era. As the entropy theory is applied to describe the energy distribution in the era of internet of things [9], power transmitted from power plants to units is just part of power need for this world, and we have to rely on energy harvested from environment. The waste of energy from human motion is one of most common dispersed energy. It is also the most convenient and efficient energy that we can harvest to supply wearable electronic by a textile-TENG, because almost all kinds of human motion can be transferred to electricity by TENG [10–15]. At the same time, wearable and flexible sensors [16–22] used in personal healthcare and bio-motion detection draw a lot of attention for their real-time, simple and effective information. So far, great progress has been made in this area [23–27]. However, textile-based TENG, there still remains challenges to face both for energy harvesting textile-TENG and TENG sensors. First, most fabric-based TENGs have several layers which are complicate to obtain and uncomfortable enough to be used in wearable devices [4,5,28–30]. Second, a majority of fabrics cannot generate electricity without contacting other fabrics or other materials [18,31]. Two fabrics or more are necessary to do contact-

∗ Corresponding authors at: School of Material Science and Engineering, Georgia Institute of Technology, Atlanta, GA 30332, United States (Z.L. Wang).
 E-mail addresses: Du, Z. (duzq@dhu.edu.cn), Wang, Z.L. (zhong.wang@mse.gatech.edu).
† These authors contributed equally to this work.

separation and contact sliding motion [32] which limits the application of fabric-based TENG. Third, the fabrication of fabric-based TENG, including coating, woven structure and composite mode, decrease the flexibility, breathability and stretchability of the fabric [33]. Forth, the uneven surface of the fabric or spun fibers may lead to the uneven surface of the coating, which cannot enable the stability of the fabric-based TENG.

Here we introduce a 3D double-faced interlock fabric triboelectric nanogenerator (3DFIF-TENG), as shown in Fig. 1a. The interlock fabric is a special structure of weft-knitted fabric, which has better flexibility, breathability and higher stretchability than woven fabric, weft plain knitted fabric and warp-knitted fabric due to special connection way of two system yarns and the freedom of the yarns in the fabric [34,35]. In this paper, the two system yarns are cotton yarn and PA (Nylon 66) composite yarn. Cotton yarn can be easy to obtain which is cost-effective. A four-ply twisted Polyamide (PA) yarn coated with Ag is used as the conductive yarn which is coated with silicone rubber to obtain the PA composite yarn. It is simple and high efficient to knit into this 3DFIF-TENG by a double needle bed flat knitting machine technology [36], which means the fabric-based TENG can be mass manufac-

tured. It is worth noting that this fabric-based TENG is substrate-free which can generate electricity by bending and stretching itself.

This work presents the 3DFIF-TENG's good electrical output performances during contact-separation operation, bend-stretch mode and only-stretch mode in transverse direction, which demonstrates the 3DFIF-TENG can be used as multifunctional wearable devices such as pressure sensor and bending sensor. Furthermore, two system yarns arrangements, cross and parallel, are compared to find a better structure design with high output performance.11 fabrics are knitted to systematically investigate the influence of triboelectric materials (6 pairs of positive and negative triboelectric materials) and structure parameters (4 different column height and 3 different column width) on the output performances of 3DFIF-TENG. A variety of applications about energy harvesting and multifunctional sensor of this fabric TENG, such as lighting up a variety of LEDs, bending sensor and weighting sensor, are introduced to exhibit its great prospect in self-powered wearable electronic devices. At last, we take advantage of the 3D structure and improve the special structure with warp inserting and weft inserting in the middle layer, which makes the 3DFIF-TENG be multifunctional as a 3D tactile sensor.
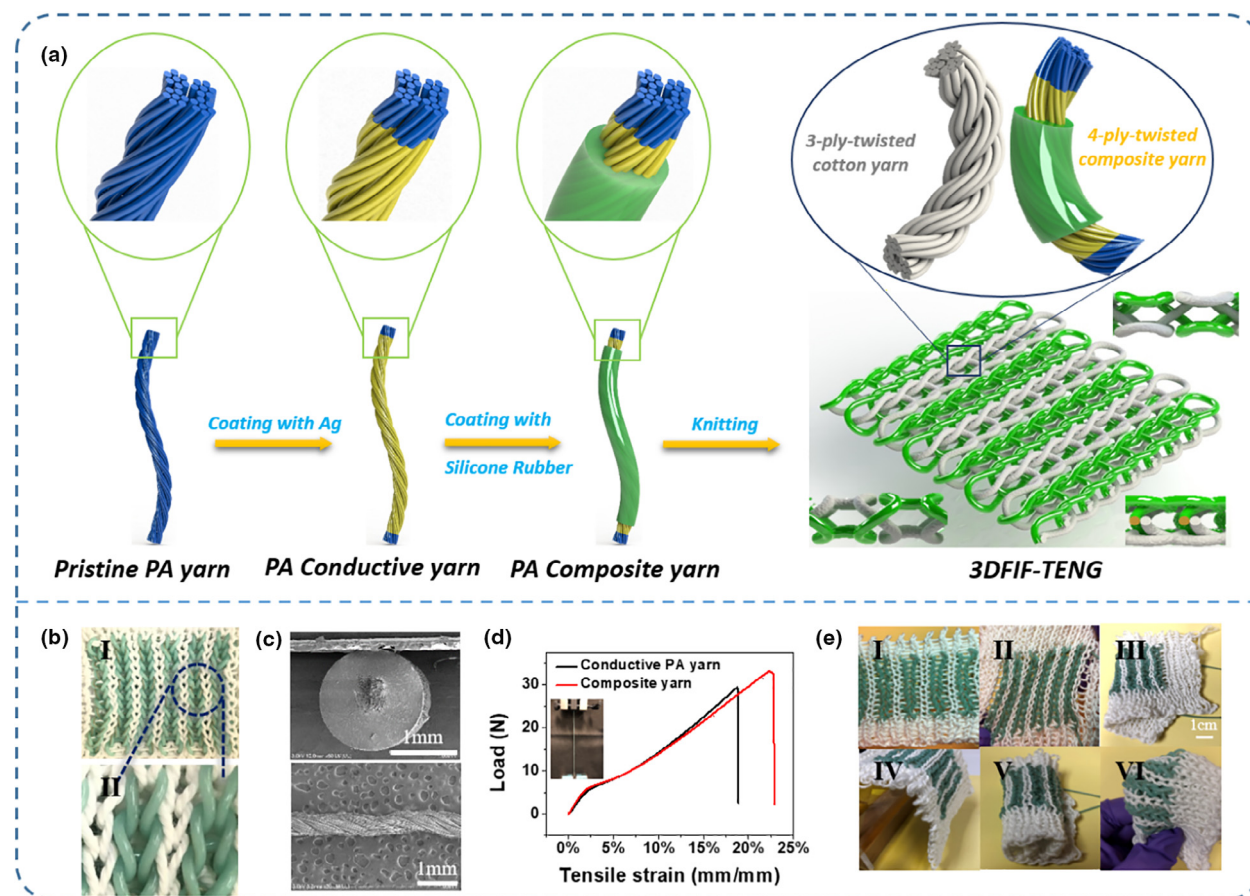
FIGURE 1

Schematic illustration, fabrication process and mechanical behavior of 3DFIF-TENG. (a) Fabrication process of the core-sheath yarn and 3DFIF-TENG. (b) Photographs of the 3DFIF-TENG (I) and the detail surface (II). (c) Cross sectional scanning electron microscopy (SEM) photographs of PA composite yarn (I) and surface SEM of conductive yarn (II), scale bar 1 mm. (d) The tensile property of the conductive yarn and PA composite yarn. (e) Photographs of 3DFIF-TENG under different deformations, including stretched (I), sheared (II), folded (III), draped (IV), crimped (V), and distorted (VI, scale bar 1 cm.

Results and discussion

The design of the TENG is presented in Fig. 1a. Cotton yarn is chosen as the positive triboelectric material, which is not only widely used in the textile industries, but it is also soft, cost-effective, breathable and comfortable. A four-ply twisted polyamide (PA) yarn coated with Ag is used as the conductive electrode because of its high conductivity. PA yarn is also a very common used textile material in the world, which has a high production and excellent performance such as high breaking strength, high elongation and high abrasive resistance. Due to the excellent flexibility and strong tendency to gain electrons of silicone rubber, the conductive yarn is coated with silicone rubber (Thickness is about 0.46 mm) to obtain the PA composite yarn.

The interlock fabric is knitted with both cotton yarn and PA composite yarn. This structure is special and different with other knitted fabrics. As show in Fig. S1 (Supplementary Data), two rib-stitch structures are knitted with each other to obtain the interlock structure. The most basic interlock structure is 1 + 1 interlock structure which is used in this paper. It is knitted by two yarns of two adjacent looping systems: one system uses cotton yarn, the other one uses PA composite yarn. Longitudinal direction loops (stitch wale) are same yarns (cotton or PA composite yarn). A rib stitch knitted by cotton yarn and the other rib stitch knitted by PA composite yarn are arranged alternately in transverse direction loops (stitch courses).

This interlock stitch is also a double-faced effect interlock structure. Cotton loop and PA composite yarn loop are back to back, that is, each cotton loop is right behind PA composite yarn loop of another face and so as to each PA composite yarn loop. Due to the special structure and the large space between adjacent yarns, this fabric TENG (area density is 168 g/m^2) has great softness, flexibility, and breathability. Any contact-separation movements, stretching (transverse and longitudinal direction) and bending operation of the fabric TENG would bring continuous alternating current outputs. Each face of the 3DFIF-TENG has the same output performance because of the double face structure, which makes the TENG more convenient to use in daily life.

Fig. 1b shows the photographs of the actual interlock fabric-based TENG (I) and its partially enlarged view (II). It is obviously that there are two lines: one is white color consisted of 3-ply-twisted cotton yarn and one is green color consisted of PA composite yarn. The cross-section of PA composite yarn (I) and the surface morphology of conductive yarn (II) observed by scanning electron microscopy (SEM) are shown in Fig. 1c. The magnified SEM images are shown in Fig. S2 (Supplementary Data). According to the Fig. S2d–f (Supplementary Data), a layer of Ag is covered on the surface of every PA fiber of the PA yarn. Hence, the electrical conductivity is very good (0.5 Ω/cm). The FE-SEM images of the coated Ag layer (thickness is about 0.25 μm) along with the cross-section of PA conductive yarn are provide in Fig. S3 (Supplementary Data). The diameter of the PA composite yarn is 1.44 mm close to the diameter of cotton yarn (1.23 mm, as shown in Fig. S4a–c, Supplementary Data). Meanwhile, the PA composite yarn is soft as cotton yarn and PA yarn, as shown in Fig. S4d (Supplementary Data), which makes the 3DFIF-TENG just look like common clothes. The tensile property of the conductive yarn and PA composite yarn are showed in Figs. 1d and

S4f (Supplementary Data). According to the tensile curves, breaking force and breaking elongation ratio of the PA composite yarn is improved compared with that of PA conductive yarn. Due to the soft texture and flexible structure of 3DFIF-TENG, it can be stretched, sheared, and bended in any direction and could withstand arbitrary complex deformations, such as crimping and distortion (Fig. 1e). For wearable electronic devices, washing ability and good breathability are essential requirements for long-term usage. Therefore, the washability and breathability (The average air permeability is 2179.85 mm/s, Table S1, Supplementary Data) of 3DFIF-TENG are tested in this work (Fig. S5, Movie S1 and Movie S2, Supplementary Data).

The double layer structure endows the 3DFIF-TENG great property in generating electricity by contacting and separating with other things, or under any arbitrary complex deformations, such as stretching (transverse and longitudinal direction), bending, shearing, crimping, and distortion operation. Therefore, it has flexible working modes. Here three working modes all belonging to single electrode mode [37–40], are adopted, as shown in Figs. 2 and S6 (Supplementary Data). For better understanding, we choose one triboelectric yarn in Fig. 2b and four triboelectric yarns in Fig. 2f to analyze the working mechanism respectively. Fig. 2a shows the two statuses of yarns which are pressed and separated corresponding to Fig. 2b-i and b-iii. Under press mode, in the original stage, no electrical potential exists between the surface of the PA composited yarn and PET film. By pressing PET film onto the fabric, the surfaces of the PA composite yarn and PET film are charged with the same amount of opposite charges (Fig. 2-b-i). The PA composite yarn is proven to be negatively charged because of silicon rubber's ability to attract more electrons than the PET film. When they are separating from each other, positive charges will be induced in the electrode (conductive yarn) by the negative charges, yielding electrons flow from the Ag through external loading to the ground (Fig. 2b-ii). As the PET film is moving quite far away, a new electrical equilibrium achieves and the electrons stop moving (Fig. 2b-iii). As the PET film approaches the silicone rubber again, electrons flow inversely from the ground to electrode (conductive yarn) to make a charge balance (Fig. 2b-iv). When the PET film fully contacts with the silicone rubber-coated yarn, charge neutralization occurs again. Continuous contact-separation movements between the PET film and the silicone rubber-coated yarn bring continuous alternating current outputs from 3DFIF-TENG through the external loading. The electrical output performances are measured by using a linear motor to provide periodic contact-separation movements (Fig. 4g). To obtain a more quantitative understanding of the electricity generating process, we establish a theoretical model of the 3DFIF-TENG to observe the electric potential distribution of PET film and PA composite yarn during the contact-separation movements by a simple finite element simulation using COMSOL Multiphasic (Fig. 2c). The V_{OC} (open-circuit voltage), I_{SC} (short-circuit current), Q_{SC} (short-circuit charge transfer) of this mode are presented in Fig. 2g when the contacted area is 25 cm^2 and the pressure is 0.4 kPa.

Since this 3DFIF-TENG can generate electricity by bending and stretching itself, the electricity generating mechanism of the fabric during stretching (in transverse direction) is discussed here. As we know, this fabric is a double-faced effect interlock
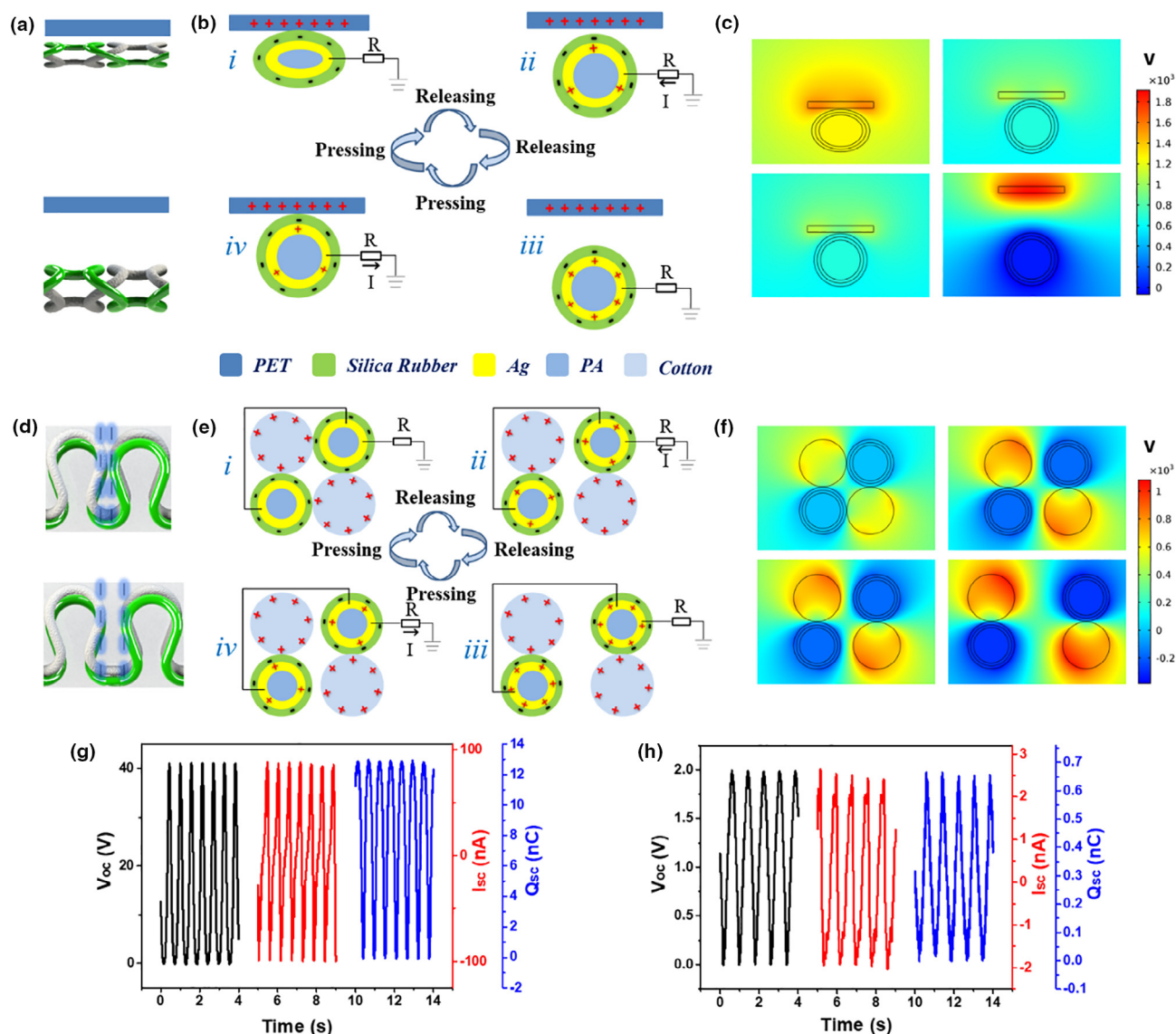
FIGURE 2

Working mechanism and electrical output performance of 3DFIF-TENG at different work situations. (a) Two statuses of 3DFIF-TENG under press. (b) Schematic diagrams of the working principles of 3DFIF-TENG under press. (c) Simulated electric field distribution of the 3DFIT-TENG under press. (d) Two statuses of 3DFIF-TENG under stretch. (e) Schematic diagrams of the working principles of 3DFIF-TENG under stretch. (f) Simulated electric field distribution of the 3DFIT-TENG under stretch. (g) Electrical output performances of 3DFIT -TENG under press. (h) Electrical output performances of 3DFIT-TENG under stretch.

structure. Cotton loops of one face are right behind the PA composite yarn loops of another face. Therefore, we choose one basic unit of cross-section in the fabric to analyze the mechanism. Fig. 2d shows the two statuses of yarns which are contacted and separated corresponding to Fig. 2e-i and e-iii. Under stretch mode, when the PA composite yarn (silicon rubber on the surface) contacts with the cotton yarn, the surfaces of the PA composite yarn and cotton yarn are charged with the same amount of opposite charges (Fig. 2e-i). The PA composite yarn is proven to be negatively charged according to the triboelectric-series table. These two surfaces are separating from each other during stretching operation, positive charges will be induced in the electrode (conductive PA yarn) by the negative charges (Fig. 2e-ii), yielding electrons flow from the Ag through external loading to

the ground. As these two surfaces are moving quite far away, a new electrical equilibrium achieves and the electrons stop moving (Fig. 2e-iii). When we stop stretching the fabric, the cotton yarn approaches the silicone rubber again, electrons flow inversely from the ground to electrode (conductive yarn) to make a charge balance (Fig. 2e-iv). When cotton yarn fully contacts with the silicone rubber-coated yarn, charge neutralization occurs again. The electrical output performances are measured by using a linear motor to provide periodic contact-separation movements. The simulated electric field distribution of 3DFIF-TENG during stretch is obtained by a simple finite element simulation using COMSOL Multiphasic (Fig. 2g). The V_{oc}, I_{sc}, Q_{sc} of this mode are presented in Fig. 1h when the length of the fabric is 5 cm and the elongation ratio is 50%. When 3DFIF-TENG is
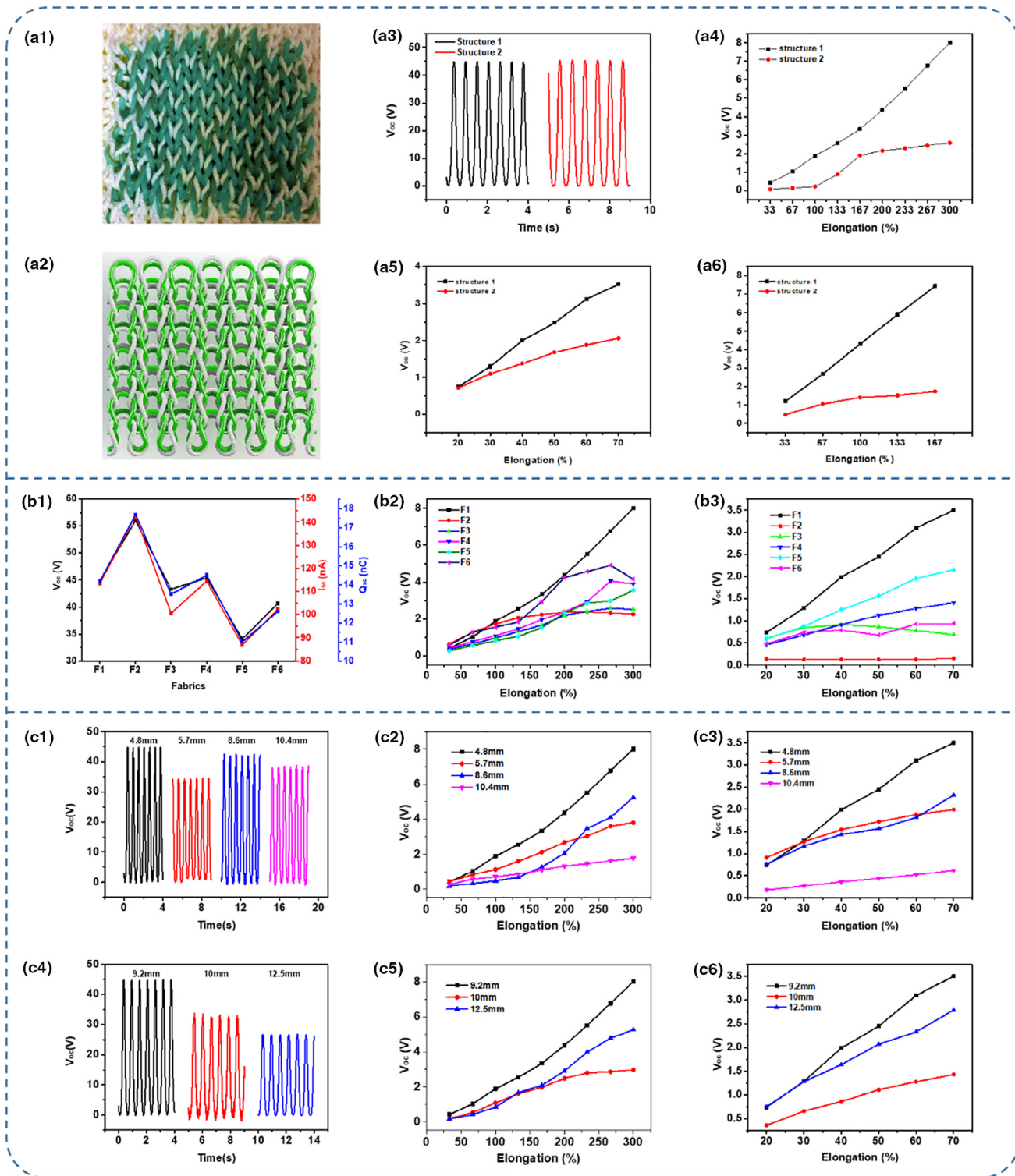
FIGURE 3

The comparison of electrical output of 3DFIF-TENG between different structures, different materials, and different structure parameters. (a1, a2) The photograph and the Schematic illustration of 3DFIF-TENG with cross loops arrangement. (a3) The V_{OC} of 3DFIF-TENG with parallel loops arrangement-Structure 1 and cross loops arrangement-Structure 2 under 2 kPa press by PET film. (a4–a5) the V_{OC} of Structure 1 and Structure 2 under bend-stretch mode, only-stretch mode in Transverse direction. (a6) The V_{OC} of Structure 1 and Structure 2 under only-stretch mode in longitudinal direction. (b1) The V_{OC}, I_{SC}, Q_{SC} of the 3DFIF-TENG (F1, F2, F3, F4, F5, F6) with 6 different materials under 2 kPa press by PET film but in same Structure 1. (b2, b3) The V_{OC} of the 3DFIF-TENG (F1, F2, F3, F4, F5, F6) under bend-stretch mode, only-stretch mode in Transverse direction. (c1) The V_{OC}, I_{SC}, Q_{SC} of the 3DFIF-TENG with 4 different column height (4.8 mm, 5.7 mm, 8.6 mm and 10.4 mm) under 2 kPa press by PET film but in same Structure 1. (c2, c3) The V_{OC} of the 3DFIF-TENG (column height: 4.8 mm, 5.7 mm, 8.6 mm and 10.4 mm) under bend-stretch mode, only-stretch mode in Transverse direction. (c4) The V_{OC}, I_{SC}, Q_{SC} of the 3DFIF-TENG with 3 different column width (9.2 mm, 10 mm and 12.5 mm) under 2 kPa press by PET film but in same Structure 1. (c5, c6) The V_{OC} of the 3DFIF-TENG (column width: 9.2 mm, 10 mm and 12.5 mm) under bend-stretch mode, only-stretch mode in Transverse direction.
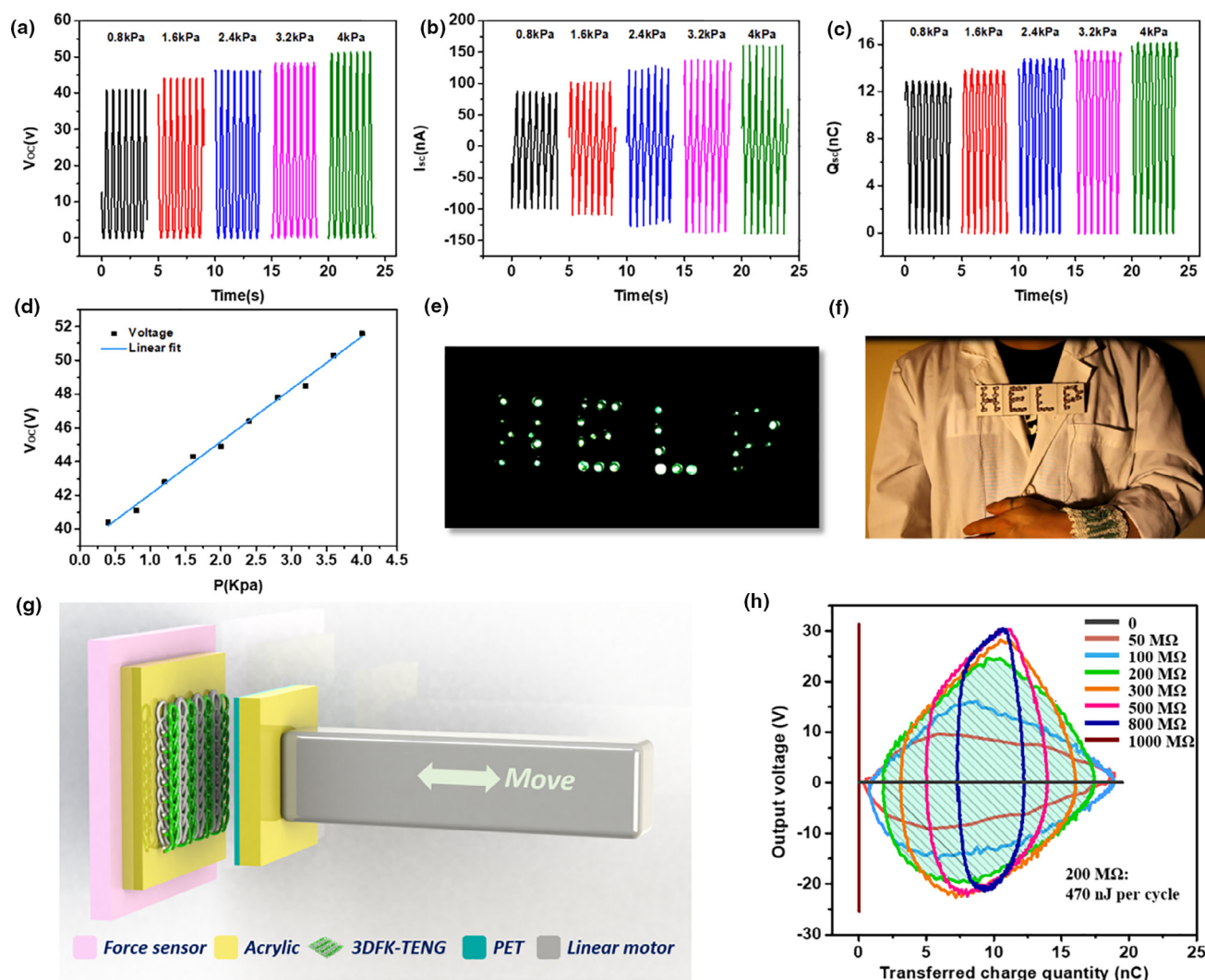
FIGURE 4

Electrical output, application and test method of the 3DFIF-TENG in press mode. (a–c) Electrical output of the fabric during contact-separation operation with increasing pressure, including (a) V_{OC}, (b) I_{SC}, (c) Q_{SC}. (d) The linear fit of the V_{OC} of 3DFIF-TENG pressed by PET film with increasing pressure from 0.4 kPa to 4 kPa. (e, f) Demonstration of lighting up LEDs marked as alphabets "HELP" by tapping the 3DFIF-TENG wrapped on the wrist. (g) Schematic diagram of the test method when the 3DFIF-TENG pressed by PET film. (h) The V-Q plot of the cycles for energy output with different external load resistance.

stretched in longitudinal direction, it would be the third working mode. And the electricity generating mechanism is shown in Fig. S6 and Note S2 (Supplementary Data).

In order to optimize the electrical output performance of 3DFIF-TENG, we change loops arrangement, structure parameters and triboelectric materials to compare their properties. In Figs. 3a-1, a-2 and S7 (Supplementary Data), the 3DFIF-TENG with cotton yarn loops and PA composite yarn loops crossed with each other (Structure 2) is designed to compare with 3DFIF-TENG with cotton yarn loops parallel to PA composite yarn loops (Structure 1, as shown in Fig. 1). From Figs. 3a-3 and S8 (Supplementary Data), under the same test condition (area is 5 cm × 5 cm; the pressure is 2 kPa), the V_{OC} of both structures is nearly the same as 45 V, and the I_{SC} and Q_{SC} of Structure 2 is a little higher than that of Structure 1. It is clearly that each cotton yarn loop is surrounded by four PA composite yarn loops, and vice versa. So the contact area between cotton yarns and PA composite yarns in Structure 2 absolutely is bigger than contact

area in Structure 1. However all test results of Structure 2 are smaller than the test results of Structure 1, including *Voc, Isc, Qsc* in Figs. 3a-4, a-5, a-6, and S9 (Supplementary Data) during bend-stretch mode, only-stretch mode in transverse direction and bend-stretch mode in longitudinal direction. Here, the test method of the bend-stretch mode, only-stretch mode will be shown in detail in Fig. 5. After observing the test process, we find that the Structure 2 is more stable and all yarn loops are stressed more evenly. However, compared with Structure 1, the full symmetry in all direction of Structure 2 would hinder the contact-separation process between cotton yarn and PA composite yarn when we stretch the fabric (Note S3). In view of output performance as TENG, Structure 1 is better. Hence we go on investigating the influence of triboelectric materials and structure parameters of 3DFIF-TENG with Structure 1 in the latter part of this article.

There are 6 kinds of 3DFIF-TENG with 6 pairs of triboelectric materials as shown in Fig. S10 (Supplementary Data). From
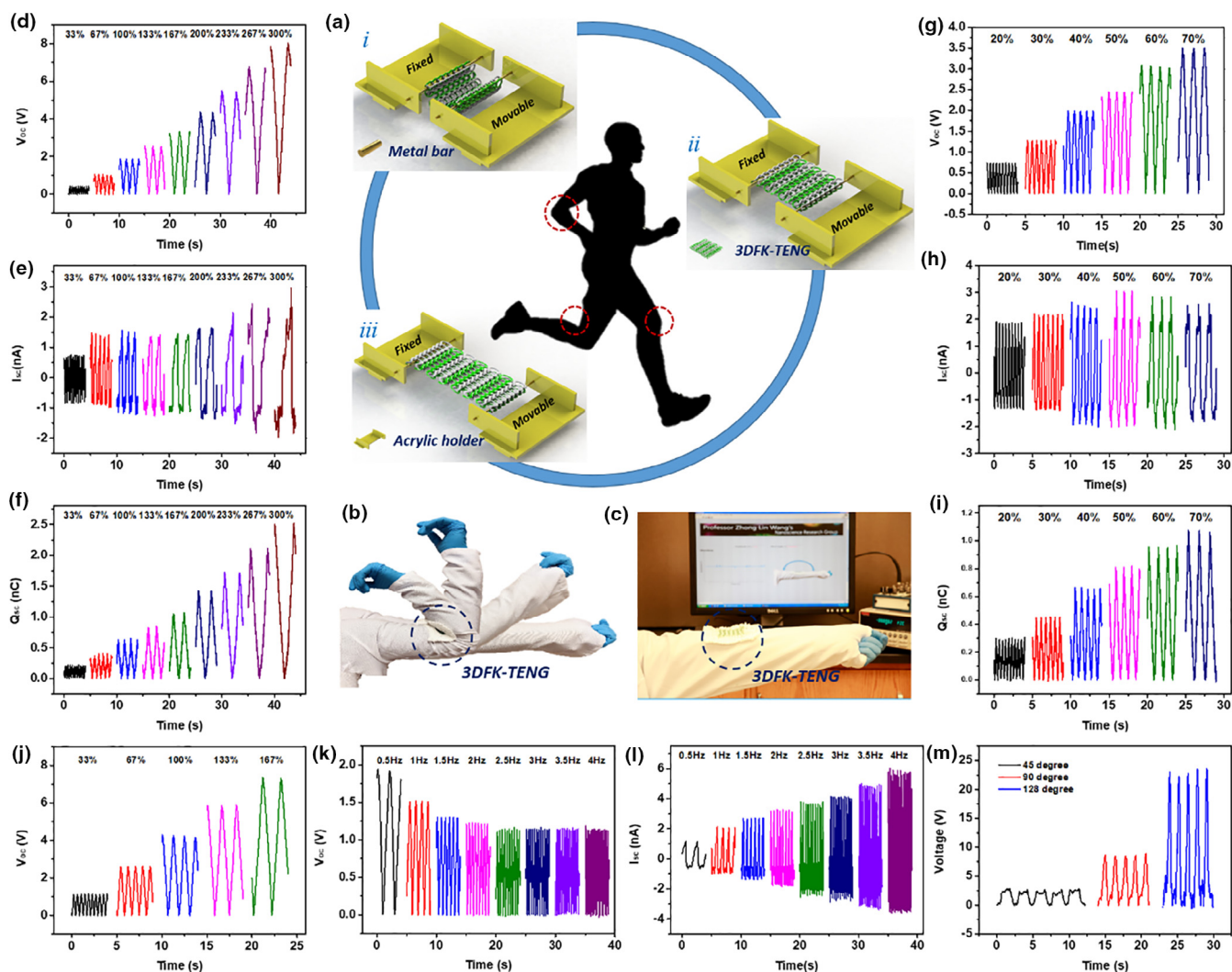
FIGURE 5

Electrical output, application and test method of the 3DFIF-TENG in stretch mode. (a) Schematic diagram of bend-stretch and only-stretch test method. (b, c) Demonstration of 3DFIF-TENG as a bending sensor to detect arm bending degree. (d–f) Electrical output of 3DFIF-TENG during bend-stretch operation at various elongation (33–300%) in transverse direction, including (d) V_{OC}, (e) I_{SC}, (f) Q_{SC}. (g–i) Electrical output of 3DFIF-TENG during only-stretch operation at various elongation (20–70%) in transverse direction, including (g) V_{OC}, (h) I_{SC}, (i) Q_{SC}. (j) The V_{OC} of 3DFIF-TENG during bend-stretch operation at various elongation (33–167%) in longitudinal direction. (k, l) The V_{OC}, I_{SC} of 3DFIF-TENG during only-stretch operation (elongation 50%) from 0.5 Hz to 4 Hz in transverse direction, including (k) V_{OC}, (l) I_{SC}. (m) The V_{OC} of 3DFIF-TENG as a bending sensor when arm bend 45°, 90° and 128°.

Fig. 3b1 and Fig. S11 (Supplementary Data), in the same test condition, fabric 2 (F2) has the biggest output performance when they are pressed by PET film under 2 kPa, which is followed by fabric 1 (F1), fabric 4 (F4), fabric 3 (F3), fabric 6 (F6) and fabric 5 (F5). From Fig. 3b2, 3b3 and Figs. S12–S15 (Supplementary Data), F1 has the best output when those fabrics are tested by bend-stretch mode, only-stretch mode in transverse direction. 4 fabrics with different column height (4.8 mm, 5.7 mm, 8.6 mm and 10.4 mm) but with almost the same column width, and 3 fabrics with different column width (9.2 mm, 10 mm and 12.5 mm) but with almost same column height are as shown in Fig. S16 (Supplementary Data). For the accuracy of the test, all these fabrics with different column height and width have the same structure 1 and the same contact-separate materials (cotton yarns and PA composite yarns). The V_{OC}, I_{SC}, Q_{SC} of these fabrics tested under 2 kPa and pressed by PET film are shown in

Fig. 3c-1, c-4 and S17 (Supplementary Data). The V_{OC}, I_{SC}, Q_{SC} of these fabrics tested under bend-stretch in transverse direction is shown in Figs. 3c-2, c-5 and S18–S21 (Supplementary Data). The V_{OC}, I_{SC}, Q_{SC} of these fabrics tested under only-stretch in transverse direction are shown in Figs. 3c-3, c-6 and S18–S21 (Supplementary Data). Comparing the V_{OC} value in Fig. 3c-1 to c-6, we find the fabric with minimum column height and column width has the maximum output. As we can see from the photographs in Fig. S16 (Supplementary Data), the fabrics which have smaller column height and column width, have cleaner, more regular contact-separate line between cotton yarns and PA composite yarns. The cleaner, more regular contact-separated line is helpful to coupling of contact charging and electrostatic induction. At last, comparing all test results of the 12 fabrics, F1 (Structure 1) turns out to be the best one, which has the minimum column height (4.8 mm) and column width
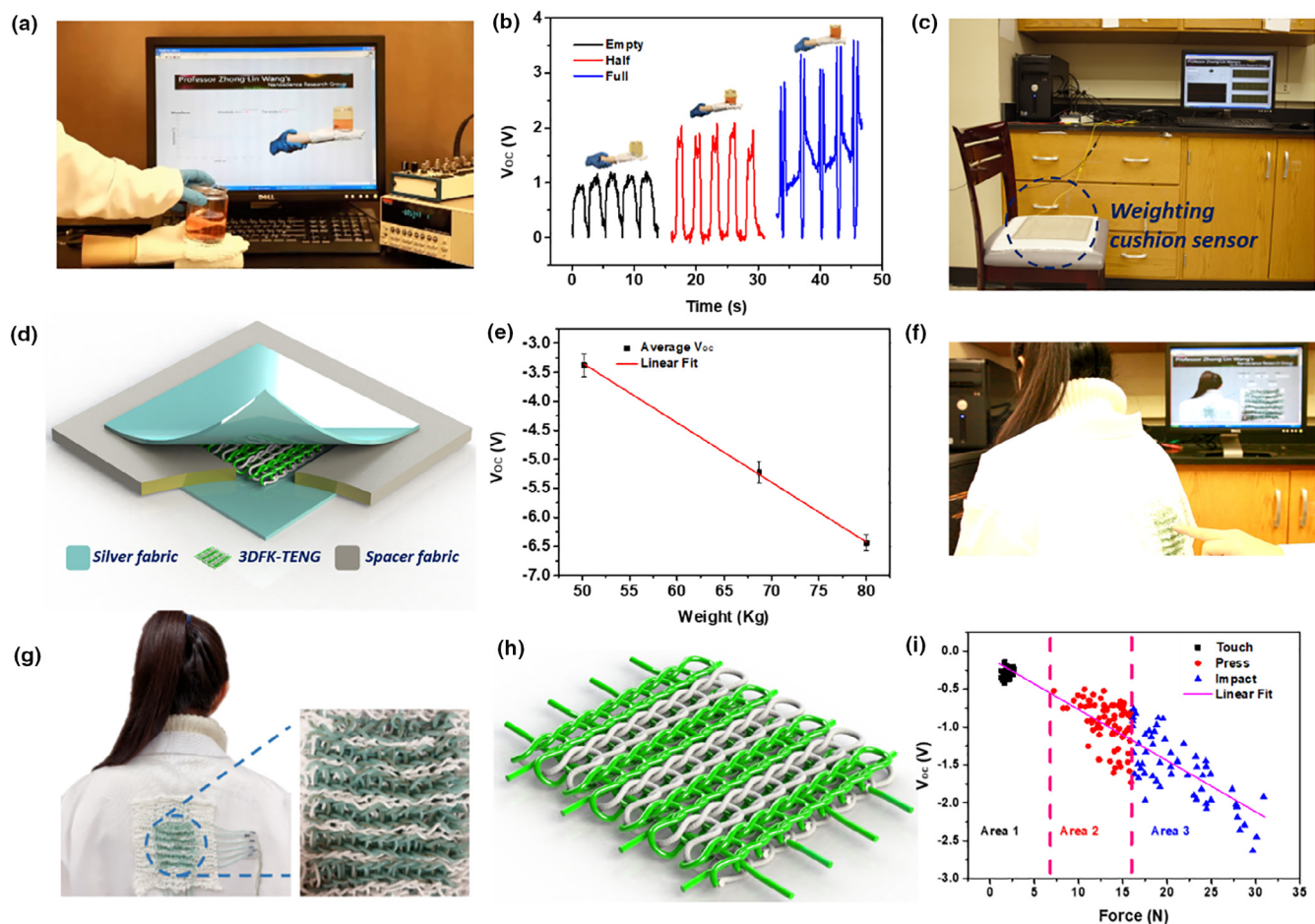
FIGURE 6

Applications of 3DFIF-TENG as a hand pressure sensor, a weighting cushion sensor, and a 3D tactile sensor. (a) Photograph of demonstration of 3DFIF-TENG as a hand pressure sensor to recognize objects with different weight. (b) The V_{OC} of 3DFIF-TENG as a hand pressure sensor when a glass bottle is empty, half of water, and full of water. (c) Photograph of demonstration of 3DFIF-TENG as a weighting cushion sensor to recognize people with weight. (d) The structure diagram of 3DFIF-TENG as a weighting cushion sensor. (e) The average V_{OC} of 3DFIF-TENG as a weighting cushion sensor when the testers' weight is 50.2 kg, 68.7 kg and 80 kg. (f) Photograph of demonstration of 3DFIF-TENG as a 3D tactile sensor to feel the location and force. (g) The photograph of 3DFIF-TENG as a 3D tactile sensor attached on the back of a tester. (h) The structure diagram of the improved 3DFIF-TENG as a 3D tactile sensor. (i) The V_{OC} of 3DFIF-TENG as a 3D tactile sensor when this sensor is pointed by a finger with different force for 160 times.

(9.2 mm) with cotton yarns and PA composite yarns as triboelectrical material. The electric output data of F1 (column height 4.8 mm and column width 9.2 mm) will be shown in detail later. And the 3DFIF-TENG we further study is F1.

As shown in Fig. 4, the properties of 3DFIF-TENG (F1) is further studied. The V_{OC} (Fig. 4b), I_{SC} (Fig. 4c) and Q_{SC} (Fig. 4d) of 3DFIF-TENG under different pressure are quantitatively measured by a mechanical linear motor (Fig. 4g). It is demonstrated that the V_{OC}, I_{SC} and Q_{SC} increase linearly with increasing pressure. The linear fit of V_{OC} (Fig. 4g) shows good linear correlation with pressure from 0.4 kPa to 4 kPa. The linear equation and more detailed data are shown in Fig. S22 (Supplementary Data). Therefore, it can be used as a pressure sensor or a weight sensor. From the V-Q plot [41] of cycles for energy output with various external load resistance (Fig. 4h), the peak energy output of 3DFIF-TENG reaches 470 nJ one circle (3.4 mW/m², Note S2, Supplementary Data) under an external load resistance of 200 MΩ. Fig. 4e and f show that the 3DFIF-TENG can sufficiently light up "HELP" sign with 35 green LEDs in series by bare hand

tapping (Movie S3, Supplementary Data). By knitting or weaving this wearable 3DFIF-TENG in clothes, we can easily harvest energy from human motion to continuously power lights and electronic products, which is important and meaningful in this world with energy shortage and serious environmental problems.

As we mentioned before, this 3DFIF-TENG can be a substrate-free textile-TENG by bending and stretching itself (Fig. 5). In Fig. 5a, during transverse direction, i—ii—iii represents a bend-stretch cycle, and ii—iii represents an only-stretch cycle. The elongation is calculated by the distance between the two metal bars. The original distance between the two metal bars is 3 cm in bend-stretch mode and 5 cm in only-stretch mode. The 3DFIF-TENG sample we use to test is 5 cm × 5 cm. Under bend-stretch mode, the V_{OC}, Q_{SC} clearly increase from 0.4 V to 8 V and 0.22 nC to 2.52 nC with the elongation increasing from 33% to 300%. But the I_{SC} basically remains constant. The V_{OC}, Q_{SC}, I_{SC} have the same trend in the only-stretch mode as shown in Fig. 5g–i. The V_{OC}, Q_{SC} get bigger because the distance between

cotton yarns and PA composite yarns increases when elongation increases. The I_{SC} remains constant because the stretch speed keeps constant at 0.05 m s^{-1}. That means the frequency will decrease when the elongation increases. In longitudinal direction, the V_{OC} (Fig. 5j), I_{SC} and Q_{SC} (Fig. S23, Supplementary Data) of only-stretch mode have the same trend with transverse direction. As shown in Figs. 5k and S23 (Supplementary Data), the V_{OC} and Q_{SC} tend to be constant (1.2 V and 0.4 nC, respectively) when the frequency increases from 0.5 Hz to 4 Hz. Nevertheless, it is obvious that the I_{SC} increases from 1.15 nA to 6.04 nA when frequency increases. Above all, the electric output of 3DFIF-TENG as a substrate-free textile-TENG changes regularly as the test parameters change in both transverse direction and longitudinal direction. The mode, direction and frequency of human motion and robot motion are changeable and complicate. Hence, compared with those bulky and rigid TENG sensor with fixed motion mode, this kind of 3DFIF-TENG has a natural advantage as a self-powered wearable bend or stretch sensor to detect human motion or robot motion. Here, we present a wearable 3DFIF-TENG sensor to detect human or robot arm bending degree. The 3DFIF-TENG sensor is attached to the inside of the elbow. According to the output V_{OC} and the curve fitting (Figs. 5m and S24) of the 3DFIF-TENG sensor, the bending degree is detected as 45°, 90° and 128° as shown in Fig. 5b, c and Movie S4 (Supplementary Data).

More applications of 3DFIF-TENG as self-powered sensors are shown in Fig. 6. The 3DFIF-TENG as hand pressure sensor is attached on the surface of a robot palm. When the output V_{OC} of this sensor range in 0.2–1.5 V, 1.5–2.5 V and 2.5–3.5 V, the glass bottle put on the palm will be recognized as empty, half bottle of water and full, as shown in Fig. 6a, b and Movie S5 (Supplementary Data). The structure diagram of weighting cushion sensor is show in Fig. 6d, where the 3DFIF-TENG is surrounded by a spacer fabrics [42–45] which has good breathability, comfort and damping property. Both the upper and lower surfaces of 3DFIF-TENG are covered with the silver fabrics, which are shielding layer to make the electric output more stable. After a female tester (50.2 kg) and a male tester (68.7 kg without a bag and 80 kg with a bag) are all tested 30 times to get the relationship between the V_{OC} and weight, which proves to be good linear correlation in Fig. 6e. The 3DFIF-TENG cushion is used as a weighting sensor in Fig. 6c and Movie S6 (Supplementary Data). This soft and comfortable cushion is also easy to take away and put on the chair in office and car.

By taking advantage of the spacer between the two layers of 3DFIF-TENG, a woven fabric-TENG (Fig. S25, Supplementary Data) is knitted into the middle layer, where the weft yarn and warp yarn are both PA composite yarns in the woven fabric-TENG. The structure diagram of this improved 3DFIF-TENG is shown in Fig. 6h and Fig. S25 (Supplementary Data). After the improved 3DFIT-TENG is pointed by a finger with different force for 160 times on a tester's back, the relationship between V_{OC} and finger force is presented in Fig. 6i. We roughly set the finger force into three feeling area: area 1(touch area), area 2(press area), and area 3(impact area). Therefore, combining with the woven fabric-TENG, the improved 3DFIF-TENG is multifunctional as a 3D tactile sensor, which can "feel" position (x,y) and force as a self-powered and wearable textile sensor, as shown in Fig. 6f

and Movie S7 (Supplementary Data). Some of the sensors shown in this paper, such as 3D tactile sensor, hand pressure sensor and bending sensor can be put on intelligent robots to make them smarter or patients who lose sensory ability to help them "feel" the world better.

Conclusion
In summary, a 3D double-faced interlock fabric triboelectric nanogenerator (3DFIF-TENG) is proposed and fabricated to harvest mechanical energy and to be used as a multifunctional sensor to monitor human movement and health. Two yarns arrangements, cross and parallel, are compared to find a better structure design with high output performance. 11 fabrics are knitted to systematically investigate the influence of triboelectric materials and structure parameters on the output performance of 3DFIF-TENG. Due to the special structure, this kind of wearable TENG can not only harvest energy from human motion to light up LEDs by tapping it with hand, but also generate electricity by bending and stretching itself without using other triboelectric materials, which can be used as self-powered multifunctional sensors. Based on the output results, the 3DFIF-TENG can be used as a bending sensor, a hand pressure sensor, a weighting cushion sensor. At last, by taking advantage of the 3D structure, we improve the special structure by knitting a woven fabric-TENG in the middle layer, which makes the 3DFIF-TENG multifunctional as a 3D tactile sensor, which can "feel" position and force as a self-powered and wearable textile sensor. This substrate-free and 3D structure design in this paper may provide a promising direction for self-powered, stretchable wearable devices.

Experimental section
Preparation of PA composite yarn
An four-ply twisted PA yarn coated with Ag is chosen as the conductive electrode and silicon rubber was chosen as the dielectric-encapsulating material to make this PA composite yarn. First, the silver-coated four-ply twisted PA conductive yarn (Jameco Electronics Inc) is inserted into a plastic tube. Second, silicon rubber (Mold Star 15 Slow, Smooth-On Inc) is prepared by mixing its two components (Part A and Part B) in a 1:1 weight ratio, and then silicon rubber is mixed with PDMS (Sylgard 184 Silicone Elastomer Base, Dow Corning Inc) in a 3:1 weight ratio. The mixture will be put it into a vacuum to eliminate the bubble. Third, inject the mixture directly into that plastic tube with silver-coated PA yarn inserted. The PA composite yarn will be obtained once the silicon rubber cure. Finally, peel off the plastic tube.

Preparation of fabric-based TENG
This 3D double-faced interlock fabric-based TENG is easily fabricated with a double needle bed flat knitting machine technology by using a miniature self-made knitting wooden loom and a bearded needle. It is knitted by two yarns of two adjacent looping systems (one system uses cotton yarn, the other one uses PA composite yarn). Longitudinal direction loops (stitch wale) are knitted by same yarns (cotton or PA composite yarn). A rib stitch knitted by cotton yarn and the other rib stitch knitted by PA

composite yarn are arranged alternately in transverse direction loops (stitch course).

Preparation of a TENG-based tactile sensor

Based on the 3D double-faced fabric-based TENG, it will be further stitched with interior warp inserting and weft inserting structure in a miniature self-made knitting wooden loom. One yarn will be inserted per two rows. The PA composite yarn is selected as the interior warp inserting and weft inserting yarn.

Methods of different tests (including bending test and stretching test)

This TENG can generate electricity by bending test and stretching itself. Therefore, we insert two metal bars into the first transverse direction loops (stitch course) and the last transverse direction loops (stitch course), respectively. One bar will be placed horizontally in the fixed acrylic holder and the other bar will be controlled horizontally by a linear motor to impose the reciprocating motion, such as bending and stretching the fabric.

Device characterizations

The surface morphology of the silver-coated PA yarn, as well as the cross-section of the PA composite yarn, was characterized by field emission scanning electron microscope (SU-8010, Hitachi). The mechanical tensile test was conducted by a universal mechanical testing machine (Model, Instron 5567). The electrical output (V_{OC}, I_{SC}, and Q_{SC}) of the fabric-based TENG during compressing, stretching and bending operation were implemented by a linear motor and an electrometer (Keithley 6514 System). The compressing and stretching forces were measured by Vernier LabQuest Mini. The air permeability of 3DFIF-TENG was tested by YG461E air permeability tester.

Acknowledgements

Appendix A. Supplementary data

Supplementary data to this article can be found online at https://doi.org/10.1016/j.mattod.2019.10.025.

References

[1] F.-R. Fan, Z.-Q. Tian, Z.L. Wang, Nano Energy 1 (2012) 328.
[2] X. He et al., Adv. Funct. Mater. 27 (2017) 1604378.
[3] J. Wang et al., Adv. Mater. 27 (2015) 4830.
[4] X. Pu et al., Adv. Mater. 28 (2016) 98.
[5] Z. Wen et al., Sci. Adv. 2 (2016) e1600097.
[6] Z.L. Wang, ACS Nano 7 (2013) 9533.
[7] G. Zhu et al., Nano Lett. 13 (2013) 847.
[8] G. Liu et al., Adv. Energy. Mater. 8 (2018) 1703086.
[9] Z.L. Wang, Nano Energy 58 (2019) 669.
[10] X. Pu et al., Sci. Adv. 3 (2017) e1700015.
[11] P. Bai et al., ACS Nano 7 (2013) 3713.
[12] K. Zhang et al., ACS Nano 9 (2015) 3521.
[13] Y.C. Lai et al., Adv. Funct. Mater. 27 (2017) 1604462.
[14] Z. Wen et al., Adv. Funct. Mater. 28 (2018) 1803684.
[15] Y. Yang et al., ACS Appl. Mater. Interfaces 10 (2018) 42356.
[16] Z.L. Wang, J. Chen, L. Lin, Energy Environ. Sci. 8 (2015) 2250.
[17] K. Dong et al., Adv. Mater. 29 (2017) 1702648.
[18] K. Dong et al., ACS Nano 11 (2017) 9490.
[19] L. Xie et al., Nano-Micro Letters 11 (2019) 39.
[20] M. Zhu et al., ACS Nano 2019 (1940) 13.
[21] T. He et al., Nano Energy 58 (2019) 641.
[22] T. He et al., Nano Energy 57 (2019) 338.
[23] Z.L. Wang et al., Mater. Today 15 (2012) 532.
[24] Q. Zheng et al., Adv. Sci. 4 (2017) 1700029.
[25] W. Paosangthong, R. Torah, S. Beeby, Nano Energy (2018).
[26] Y. Hu, Z. Zheng, Nano Energy 56 (2019) 16.
[27] Q. Shi, T. He, C. Lee, Nano Energy 57 (2019) 851.
[28] A.Y. Choi et al., Sci. Rep. 7 (2017) 45583.
[29] S.S. Kwak et al., ACS Nano 11 (2017) 10733.
[30] S. Li et al., Adv. Energy. Mater. 7 (2017) 1602832.
[31] Y. Song et al., Appl. Phys. Lett. (2017) 111.
[32] A. Yu et al., ACS Nano 11 (2017) 12764.
[33] K. Dong et al., Adv. Mater. 30 (2018) 1804944.
[34] M.J. King, P. Jearanaisilawong, S. Socrate, Int. J. Solids Struct. 42 (2005) 3867.
[35] M. Matsuo, T. Yamada, Text. Res. J. 79 (2009) 275.
[36] W. Choi, N.B. Powell, J. Textile Apparel Technol. Manage. 4 (2005) 1.
[37] Y. Yang et al., Adv. Mater. 25 (2013) 6594.
[38] S. Niu et al., Adv. Funct. Mater. 24 (2014) 3332.
[39] Z.L. Wang, Mater. Today 20 (2017) 74.
[40] X. Wang et al., Adv. Mater. 29 (2017) 1605817.
[41] Y. Zi et al., Nat. Commun. 6 (2015) 8376.
[42] Z. Du, H. Hu, Text. Res. J. 82 (2012) 1569.
[43] C. Chen et al., Text. Res. J. (2017). 0040517517690628.
[44] C. Chen et al., Text. Res. J. (2017). 0040517517690630.
[45] C. Chen et al., Text. Res. J. (2016). 0040517516676060.